ResearchGate

See discussions, stats, and author profiles for this publication at: https://www.researchgate.net/publication/230702161

Biocompatible Poly(2-hydroxyethyl methacrylate)-b-poly(L-histidine) Hybrid Materials for pH-Sensitive Intracellular Anticancer Drug Delivery

ARTICLE *in* ADVANCED FUNCTIONAL MATERIALS · MARCH 2012

Impact Factor: 11.81 · DOI: 10.1002/adfm.201102756

CITATIONS
46

READS
109

8 AUTHORS, INCLUDING:

Renjith P Johnson
University of South Carolina
21 PUBLICATIONS **118** CITATIONS
SEE PROFILE

Young-Il Jeong
Pusan National University
183 PUBLICATIONS **3,682** CITATIONS
SEE PROFILE

Sae-Ock Oh
Pusan National University
45 PUBLICATIONS **535** CITATIONS
SEE PROFILE

Hongsuk Suh
Pusan National University
201 PUBLICATIONS **3,147** CITATIONS
SEE PROFILE

Available from: Renjith P Johnson
Retrieved on: 26 January 2016

ADVANCED FUNCTIONAL MATERIALS
www.afm-journal.de

Biocompatible Poly(2-hydroxyethyl methacrylate)-*b*-poly(L-histidine) Hybrid Materials for pH-Sensitive Intracellular Anticancer Drug Delivery

*Renjith P. Johnson, Young-Il Jeong, Eunji Choi, Chung-Wook Chung, Dae Hwan Kang, Sae-Ock Oh, Hongsuk Suh, and Il Kim**

A series of synthetic polymer bioconjugate hybrid materials consisting of poly(2-hydroxyethyl methacrylate) (p(HEMA)) and poly(L-histidine) (p(His)) are synthesized by combining atom transfer radical polymerization of HEMA with ring opening polymerization of benzyl-*N*-carboxy-L-histidine anhydride. The resulting biocompatible and membranolytic p(HEMA)$_{25}$-*b*-p(His)$_n$ (n = 15, 25, 35, and 45) polymers are investigated for their use as pH-sensitive drug-carrier for tumor targeting. Doxorubicin (Dox) is encapsulated in nanosized micelles fabricated by a self-assembly process and delivered under different pH conditions. Micelle size is characterized by dynamic light scattering (DLS) and transmission electron microscopy (TEM) observations. Dox release is investigated according to pH, demonstrating the release is sensitive to pH. Antitumor activity of the released Dox is assessed using the HCT 116 human colon carcinoma cell line. Dox released from the p(HEMA)-*b*-p(His) micelles remains biologically active and has the dose-dependent capability to kill cancer cells at acidic pH. The p(HEMA)-*b*-p(His) hybrid materials are capable of self-assembling into nanomicelles and effectively encapsulating the chemotherapeutic agent Dox, which allows them to serve as suitable carriers of drug molecules for tumor targeting.

1. Introduction

The creation of bioconjugates by combining polymers with peptides and proteins is an emerging multidisciplinary field of research that has been attracting increasing attention within the scientific community. These chimera molecules combine the precise chemical structures and functionalities of biomolecules with the stability and processibility of synthetic polymers. Importantly, block copolymers composed of polypeptide segments have shown significant advantages in controlling the functional and supramolecular structures of bioinspired self-assemblies in aqueous solution.[1] The amphiphilic character of these peptide–polymer conjugates may enable them to self-assemble into functional, bimolecular materials, and they have been developed as drug-delivery systems[2] in biotechnology[3] and as sensors.[4] Moreover, these "smart" materials can change their physiochemical properties in response to variations in temperature,[5] pH,[6] or ionic strength.[7]

Polymer bioconjugates can generally be defined as synthetic macromolecules covalently linked to biological moieties. Usually, block co-polypeptides are synthesized in one of two ways: 1) the ring-opening polymerization (ROP) of *N*-carboxyanhydride (NCA) initiated by an amino-terminated polymer chain or by a transition metal based catalyst or 2) solid- or solution-phase peptide synthesis and subsequent coupling to a carboxyl-terminated polymer. Nowadays, controlled radical polymerization techniques are successfully combined with ROP to obtain block copolymers containing peptide blocks.[8] The most common homo-polypeptides are based on glutamic acid and lysine as these are known to provide the best-controlled products, but several other kinds of polypeptides have also been reported.[9] Studies carried out on the synthesis of peptide-based block copolymers, special focus was given to the evaluation of the influence of non-peptide block chemistry on peptide block organization.[10] For non-peptide block, semicrystalline, amorphous, hydrophilic, hydrophobic, and π-conjugated polymers, for example, poly(ethylene oxide)[11]

R. P. Johnson, E. Choi, Prof. I. Kim
The WCU Center for Synthetic Polymer Bioconjugate Hybrid Materials
Department of Polymer Science and Engineering
Pusan National University
Pusan 609-735, Korea
E-mail: ilkim@pusan.ac.kr
Dr. Y.-I. Jeong, Dr. C.-W. Chung, Prof. D. H. Kang
National Research and Development Center for Hepatobiliary Cancer
Pusan National University
Yangsan Hospital
Yangsan 626-870, Korea
Prof. S.-O. Oh
Department of Anatomy
Pusan National University
Yangsan 626-870, Korea
Prof. H. Suh
Department of Chemistry and Chemistry Institute for Functional Materials
Pusan National University
Pusan 609-735, Korea

DOI: 10.1002/adfm.201102756

© 2012 WILEY-VCH Verlag GmbH & Co. KGaA, Weinheim

poly(*N*-isopropylacrylamide),[12] poly(dimethylsiloxane),[13] poly(styrene),[14] poly(butadiene),[15] poly(isoprene),[16] and poly(fluorine)[17] have been used as macroinitiators.

The interesting properties of poly(2-hydroxyethyl methacrylate) (p(HEMA)) make it an important system. The p(HEMA) structure permits a water content similar to that of living tissue, and p(HEMA)-based systems exhibit excellent biocompatibility and good blood compatibility.[18] Other biomedical applications for HEMA-based materials include embedding substrates for the examination of cells using light microscopy[19] and inert matrices for the slow release of drugs.[20] Incorporation of poly(L-histidine) (p(His)) as a peptide block has also attracted considerable attention because of its nontoxic nature, biocompatibility, nutritional functions, and pharmacological efficiency as drug carriers. p(His) is known to show endosomal membrane-disruption activity, which is induced by the "proton sponge" mechanism of the imidazole groups.[21] Furthermore, the imidazole group in the histidine residue can be easily protonated to yield a positively charged residue and can also form stable polyion complexes with negatively charged polymers such as DNA oligodeoxynucleotide or enzymes. Biodegradable polyion complexes of this type have been studied as carriers for genetic material.[22] Thus, the polymeric micelle system with a p(His) core could be an effective mode for the controlled delivery of drug molecules. In general, drugs are physically loaded within the cores of polymeric micelles or chemically conjugated with poly(amino acid)s with subsequent polymeric micelle formation.[23]

Here, we focus on a new bioconjugate hybrid materials based on a hydrophilic corona-forming p(HEMA) as the synthetic polymer segment and pH-sensitive p(His) as the core-forming biopolymer block. Recently, we reported both the aspect of molecular architecture control of chain growth and the pattern of chain growth by the utilization of a trifunctional initiator for the sequential polymerization of styrene and γ-benzyl-L-glutamate-NCA.[24] To the best of our knowledge, the use of end-functionalized p(HEMA) as a macroinitiator for the controlled ROP of NCAs has not been reported yet. In this contribution, we propose a synthetic protocol of a new series of bioconjugate diblock copolymers using end-functionalized p(HEMA) as a macroinitiator, which permits the silazane-mediated controlled polymerization of benzyl-*N*-carboxy-L-histidine anhydride (His-NCA). We fabricated nanosized micelles by the self-assembly of these block polymers and encapsulated doxorubicin (Dox) for the evaluation of the drug-loading and drug-release behaviors in various pH conditions. Cytotoxicity of the micelles were tested with embryonic kidney 293T cells and HCT116 cell lines. The pH- and dose-dependent antitumor effect of released Dox has also been investigated in vivo using HCT 116 human colon carcinoma cells.

2. Results and Discussion

2.1. Polymerization of HEMA

Hydrophilic p(HEMA) is one of the most widely using biocompatible polymer in various biomedical applications, such as tissue engineering, soft contact lenses, and drug delivery systems.[25] The main criterion for selection of p(HEMA) as the basic component is its biocompatibility. p(HEMA) contains hydroxyl groups on its surfaces. Its hydrophilic surface has a low interfacial free energy in contact with body fluids, which results in a low tendency of proteins and cells to adhere to these surfaces. HEMA cannot be polymerized by anionic or group-transfer polymerization because of the labile proton on the hydroxyl group. There have been several reports on the synthesis of HEMA-based block copolymers by anionic polymerization, but this approach requires the protection of the alcohol functionality.[26] Such a synthesis involves many steps, including protection, polymerization, and subsequent removal of the protecting groups. Since its discovery,[27] atom transfer radical polymerization (ATRP) has been shown to be a versatile technique for the controlled polymerization of many classes of monomers including acrylates, methacrylates, and styrenics.[28] Weaver et al.[29] reported the synthesis of a range of p(HEMA)s and HEMA-based copolymers with controlled structure using ATRP in methanol. Because of its high molecular weight (MW), p(HEMA) is not very soluble in aqueous media and a reduction of its MW is needed to render it soluble in aqueous environments. Consequently, in this work we focus on ways to synthesize p(HEMA)s with discrete MW and low polydispersity index (PDI).

HEMA was polymerized using ethyl 2-bromoisobutyrate (BriB) as an ATRP initiator. Polymerization was conducted at a HEMA: methanol ratio of 1:2 (w/w) with the 2,2′-bipyridine (bpy) ligand, and CuBr was used to form the catalyst complex. The polymerization data are summarized in Table S1 (Supporting Information). p(HEMA)s of low MW could be produced by simply tuning the monomer to initiator ratio in high yield within a short period of polymerization. Thus, the well-controlled polymerization of HEMA is possible under mild and industrially attractive conditions. A value of MW was obtained by gel permeation chromatography (GPC), indicating an overestimation, which is typically rationalized on the basis of different hydrodynamic radii of p(HEMA) and PS standards used in GPC. Beers et al. also reported significant differences between their GPC data and their target molecular weights.[30] This discrepancy was presumably due to calibration errors in the GPC analysis because PS standards are not likely to be reliable for the analysis of p(HEMA). On the basis of a single methyl methacrylate-HEMA diblock copolymer synthesis Beers et al. estimated that their GPC protocol overestimated the true molecular weight by a factor of 2. Unfortunately, insufficient details were provided to enable us to make a close comparison with our own GPC protocol. However, based on the NMR-derived number average molecular weight (M_n) data presented in Table S1 (Supporting Information), which is almost in line with theoretical values, GPC analysis appears to overestimate the true MW of p(HEMA) by a factor of about 3. We chose $p(HEMA)_{25}$ as a representative sample for further chemistry.

2.2. End-Capping of $p(HEMA)_{25}$-Br

For the synthesis of p(HEMA)-*b*-p(His) by the ROP of His-NCA, the bromine-terminated p(HEMA) should first be functionalized

© 2012 WILEY-VCH Verlag GmbH & Co. KGaA, Weinheim

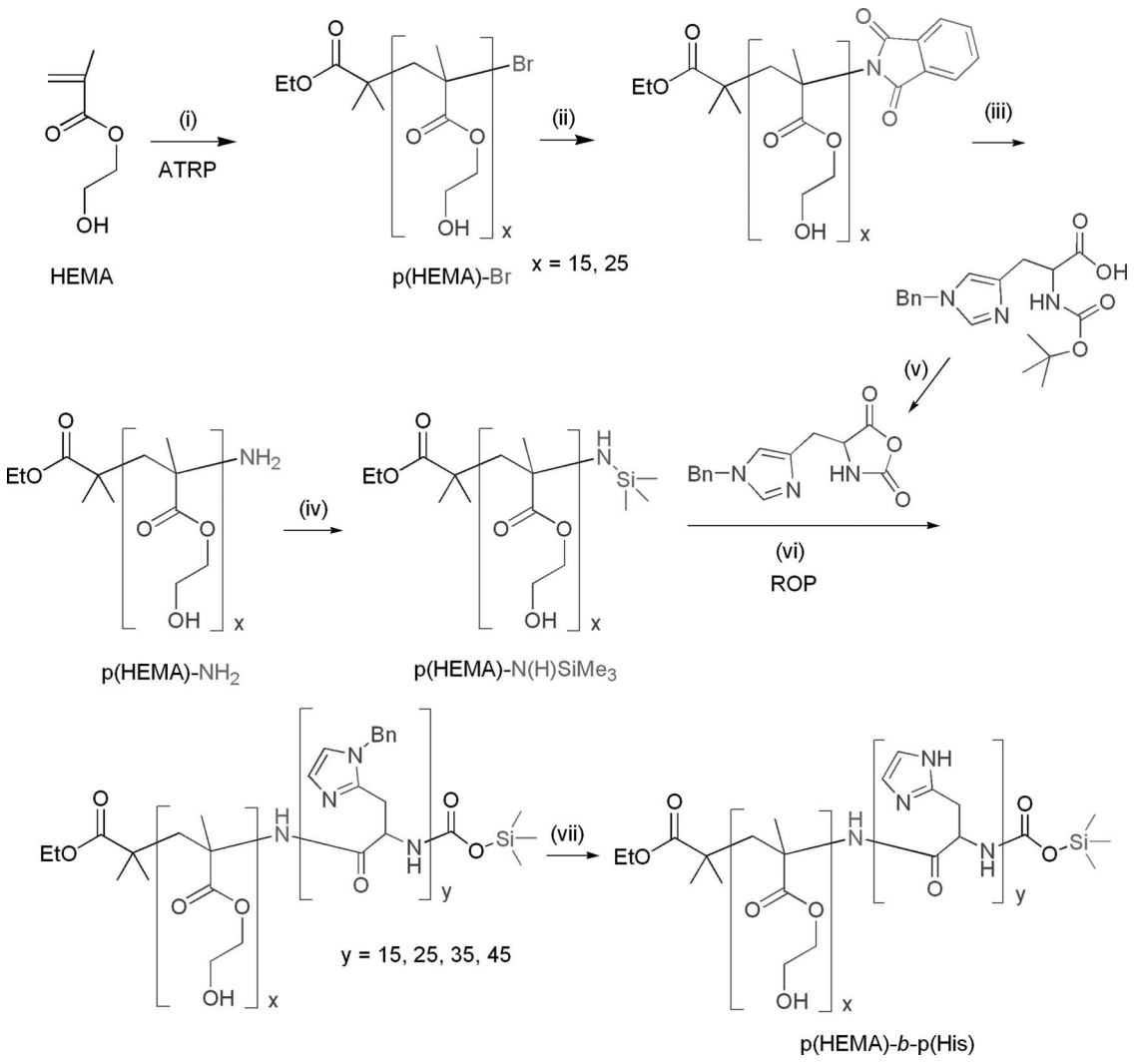

Scheme 1. Synthesis procedures of p(HEMA)-*b*-p(His) by combining ATRP of HEMA with ROP of Bz-His-NCA, followed by deprotection: i) ethyl 2-bromoisobutyrate, Cu(I)Br, bpy; ii) phthalimide potassium salt, DMF, reflux; iii) KOH, tBuOH, reflux; iv) N,O-bis(trimethylsilyl)acetamide, DMF, room temperature (r.t.); v) PCl5, 1,4-dioxane; vi) DMF, r.t.; and vii) HBr/AcOH, TFA; 0 °C.

to amine groups, since amine functionalized polymer can utilized as a macroinitiator for the synthesis of polypeptide-containing block co-polymers. Gabriel's reaction was found to be an efficient method for the conversion of halogen end groups to amino groups of polyacrylates without using toxic chemicals such as sodium azide. In the first step, the terminal bromine is displaced by nucleophilic substitution using the phthalimide potassium salt in refluxing *N,N*-dimethylformamide (DMF) (**Scheme 1**). The primary amine is then isolated after hydrolysis with potassium hydroxide in refluxing *t*-BuOH. All the products were characterized by ^{1}H NMR and Fourier transform infrared (FTIR) spectroscopy (Figure S1,S2, Supporting Information). The phthalimide end-capped p(HEMA) shows characteristic signals at 7.5–7.7 ppm that are attributable to the phthalimide group. The primary amine shows a characteristic signal at 4.5 ppm. Note that the M_n of the polymer was determined from the intensity ratios of the p(HEMA) methylene protons (at 3.81 ppm) and the phthalimide protons (at 7.5–7.7 ppm). The infrared (IR) spectra indicate the presence of amide carbonyl groups with peaks at 1776 cm^{-1} and 1725 cm^{-1} that are absent in p(HEMA)$_{25}$-Br. Finally, the spectrum of the primary-amine-terminated p(HEMA) shows the appearance of a strong band at around 3000 cm^{-1} corresponding to the amine, whereas the amide carbonyl band at 1776 and 1725 cm^{-1} has disappeared.

In recent decades, several NCA polymerizations have been reported using different initiators such as conventional amines and/or transition metal complexes.[31] On the basis of the previous work on NCA polymerizations, it was concluded that certain weak points exist. The syntheses of homo and block polypeptides with low polydispersities were unsuccessful because of unwanted side reactions. Transition-metal-mediated NCA polymerizations led to polypeptides with low PDIs; however, tedious synthesis procedures and the separation of the transition metal from the polymer are drawbacks. Ammonium-mediated polymerizations[32] and the application of high-vacuum techniques[33] allow the preparation of

© 2012 WILEY-VCH Verlag GmbH & Co. KGaA, Weinheim

Table 1. Results of ring opening polymerization of Bn-His-NCA by using p(HEMA)-*N*-TMS-amine as a macroinitiator for the synthesis of p(HEMA)-*b*-p(His). Polymerization conditions: p(HEMA)-*N*-TMS-amine = 0.45 g (0.15 mmol), DMF = 10 mL, temperature = 20 °C, and time = 48 h.

Theoretical composition	Bn-His-NCA [mmol]	Yield [%]	M_n[a] $\times 10^{-3}$ [g mol^{-1}]			NMR composition	PDI[c]
			Theoretical[b]	NMR	GPC		
p(HEMA)$_{25}$-*b*-p(His)$_{15}$	2.25	62	5.05	4.80	11.0	p(HEMA)$_{25}$-*b*-p(His)$_{13}$	1.20
p(HEMA)$_{25}$-*b*- (His)$_{25}$	3.75	59	6.42	6.22	16.0	p(HEMA)$_{25}$-*b*- p(His)$_{23}$	1.21
p(HEMA)$_{25}$-*b*-p(His)$_{35}$	5.25	63	7.79	7.24	20.0	p(HEMA)$_{25}$-*b*- p(His)$_{30}$	1.26
p(HEMA)$_{25}$-*b*-p(His)$_{45}$	6.75	66	9.16	8.72	24.7	p(HEMA)$_{25}$-*b*- p(His)$_{41}$	1.28

[a] Number average molecular weight measured after deprotecting benzyl groups; [b] M_n (theoretical) = {([Bn-His-NCA]$_0$/[p(HEMA)-*N*-TMS-amine]$_0$) × (MW of repeating unit after deprotecting benzyl group) + (MW of initiator)}. Conversion was assumed to be 100%; [c] Polydispersity index measured by GPC.

polypeptides with low PDI; however, again, tedious preparation and workup procedures are needed. Recently, Lu et al.[34] showed the highly effective silazane-mediated polymerization of α-amino acid NCA with different *N*-trimethylsilylamine (*N*-TMS-amine) functionalized initiators. In order to employ this protocol, p(HEMA)$_{25}$-NH$_2$ was further modified to a secondary amine moiety by reaction with *N,O*-bis(trimethylsilyl)-acetamide (BSA) in DMF (see Scheme 1). The obtained p(HEMA)$_{25}$-*N*-TMS-amine shows the characteristic signal at 0.01 ppm attributable to the *N*-TMS group, and other signals specific to polymer main-chain protons. In addition, the IR spectrum of p(HEMA)$_{25}$-*N*-TMS amine show a Si–N band at 850 cm^{-1}, and the presence of a N–H band at 3000 cm^{-1} confirms the complete terminal functionalization of the initiator (also see Supporting Information).

2.3. Synthesis of p(HEMA)$_{25}$-*b*-p(His)$_n$ (*n* = 15, 25, 35, 45)

The ROP of Bn-His-NCA (Bn = benzyl) was performed using the p(HEMA)$_{25}$-*N*-TMS macroinitiator (see Scheme 1). These polymerizations progress via the TMS carbamate propagating group and involve cleavage of the Si–N bond of the initiator during the initiation step. When *N*-TMS-amine is used as the initiator, polypeptide chain transfer through the "activated monomer mechanism" is eliminated; chain propagation can only proceed through the ring-opening reaction at the CO-5 position of NCA, resembling ammonium-mediated NCA polymerization but occurring much more quickly. *N*-TMS-amine mediated polymerizations result in quantitative monomer conversion and do not require any catalysts or activators to facilitate the reactions. All the polymerizations were completed within 48 h at mild conditions to yield p(HEMA)$_{25}$-*b*-p(Bn-His)$_n$ (*n* = 15, 25, 35, and 45).

The benzyl protective side chains were removed by treating p(HEMA)$_{25}$-*b*-p(Bn-His)$_n$ with HBr/AcOH in trifluoroacetic acid, and the resulting block copolymer was characterized by ^{1}H, ^{13}CNMR and FTIR spectroscopy (see Figure S4,S5, and S9 in the Supporting Information). After the deprotection of Bn moiety, the peak integral ratio of the methylene proton of p(HEMA) (δ = 3.8 ppm) and (O=C–CH–) in the peptide block (δ = 4.95 ppm) was used to calculate M_n, confirming that there was neither loss of the histidine repeating units by backbone scission nor cleavage of the peptide segments during deprotection. Therefore, we can ascertain that the polymerization of Bn-His-NCA and deprotection of benzyl groups are successfully accomplished by using the *N*-TMS-amine functionalized p(HEMA). The polydispersity of the block copolymers is around 1.20, and the M_n value is close to that predicted from the initial monomer/macroinitiator ratio (**Table 1**). The differences between the GPC data and the target MWs were also observed for the block copolymers presumably due to calibration errors in the GPC analysis.[30] GPC curves of p(HEMA)-*b*-p(His) are shown in Figure S3 of the Supporting Information.

2.4. Self-Assembly of p(HEMA)-*b*-p(His) in Aqueous Solution

It is well known that in certain solvents, that is, thermodynamically favorable solvents for one block and precipitants for the other block copolymers associate and form micellar aggregates.[35] Polymeric micelles hold a significant potential as drug delivery vehicles for a wide array of anticancer drugs due to their unique properties, such as high solubility, high drug loading capacity, and low toxicity. The micelles consist of a rather swollen core of insoluble blocks surrounded by a protective corona of soluble blocks. Recent studies on the self-assembly of polypeptides in aqueous environments have concentrated on determining the influences of various parameters such as molecular weight, solvent, temperature, salt, pH, and amino acid composition.[35] These parameters affect the aggregation behavior and lead to a variety of micellar morphologies. To confirm their self-arrangement and encapsulation capabilities, all four samples of diblock copolymers shown in **Table 2** were evaluated for micelle formation via a self-assembly process. The formation of micellar nanoparticles was confirmed by dynamic light-scattering (DLS) and finally by transmission electron microscopy (TEM) observations. Furthermore the self-assembly was also monitored by ^{1}H NMR spectroscopy. ^{1}H NMR spectras were recorded in a deuterated form of dimethyl sulfoxide (DMSO-d_6) and DMSO-d_6/D$_2$O mixtures (Figure S10, Supporting Information). The intensity of the signals assigned to the p(His) block decreases by gradually increasing the amount of D$_2$O, indicating the micelles consist of the hydrophobic p(His) core and the hydrophilic p(HEMA) corona. As shown in **Figure 1**, the micelles formed were well dispersed and displayed spherical morphology. They were uniform in size, with an average diameter of approximately 100–120 nm. The prepared micelles were found to be stable over the temperature

© 2012 WILEY-VCH Verlag GmbH & Co. KGaA, Weinheim

Table 2. Average diameter and its distribution of p(HEMA)-*b*-p(His) micelles fabricated by self-assembly before and after Dox encapsulation, and the resulting drug loading content (DLC) and drug loading efficiency (DLE).

Sample	pH	Blank micelles		Dox-loaded micelles at 20:1 (w/w)[a)]			
		Cumulant diameter	Particle size distribution	Cumulant diameter	Particle size distribution	DLC [%]	DLE [%]
$p(HEMA)_{25}$-*b*-$p(His)_{15}$	7.4	110.1 ± 0.9	0.21 ± 0.01	123.8 ± 3.2	0.29 ± 0.03	7.8	31
	6.8	132.4 ± 0.7	0.46 ± 0.04	165.2 ± 1.6	0.38 ± 0.09		
	6.5	166.5 ± 0.4	0.73 ± 0.07	214.1 ± 1.9	0.41 ± 0.06		
	6	289.1 ± 0.5	0.65 ± 0.06	544.3 ± 2.2	0.58 ± 0.05		
$p(HEMA)_{25}$-*b*-$p(His)_{25}$	7.4	98.9 ± 1.4	0.23 ± 0.01	118.1 ± 3.2	0.16 ± 0.04	8.5	34
	6.8	121.5 ± 0.9	0.19 ± 0.03	151.5 ± 2.1	0.25 ± 0.09		
	6.5	180.3 ± 2.1	0.31 ± 0.07	210.2 ± 1.3	0.62 ± 0.02		
	6	324.1 ± 1.6	0.92 ± 0.06	513.3 ± 4.9	0.73 ± 0.01		
$p(HEMA)_{25}$-*b*-$p(His)_{35}$	7.4	128.8 ± 1.8	0.16 ± 0.06	155.1 ± 2.4	0.21 ± 0.03	10.4	41
	6.8	152.3 ± 2.2	0.18 ± 0.02	234.1 ± 3.2	0.32 ± 0.08		
	6.5	254.0 ± 2.6	0.26 ± 0.07	317.0 ± 2.8	0.45 ± 0.09		
	6	382.1 ± 3.8	0.45 ± 0.06	528.0 ± 6.9	0.58 ± 0.05		
$p(HEMA)_{25}$-*b*-$p(His)_{45}$	7.4	152.3 ± 0.9	0.21 ± 0.06	194.1 ± 0.9	0.16 ± 0.03	11	44
	6.8	174.1 ± 1.9	0.38 ± 0.05	331.3 ± 1.6	0.26 ± 0.09		
	6.5	214.0 ± 1.3	0.47 ± 0.46	387.4 ± 4.2	0.39 ± 0.89		
	6	416.1 ± 1.7	0.52 ± 0.06	634.3 ± 5.1	0.48 ± 0.59		

[a)]Feed ratio of polymer to Dox. All measurements were performed in triplicate at 37 °C.

range 20–50 °C and showed no appreciable change in their size distributions (evaluated from the DLS measurements).

2.5. Loading and Release of Dox

To completely understand the potential of the self-assembled micelles of p(HEMA)-*b*-p(His) for use in drug-delivery systems, we used Dox, a chemotherapeutic drug| that is given to treat many different types of cancer. To determine their drug loading and release properties, Dox was encapsulated in the copolymer micelles by the dialysis method. As summarized in Table 2, the size and size distributions of the Dox-loaded micelles were larger than those of the blank micelles. Highly uniform overall and textual morphologies remained basically unchanged after Dox encapsulation (Figure 1e,f). The drug-loading capacity of the micelles increases slightly with increasing length of the peptide block. For linear polymers the hydrophobic drug is surrounded in the core by individual polymer chains. However, both inter-and intramolecular hydrophobic interactions may contribute to the drug encapsulation leads to improved drug loading capacity and efficiency.

Release of Dox from the micelles was observed for 100 h, and the release performance of Dox was traced using a UV-vis spectrometer. The Dox release profiles are illustrated in **Figure 2**. The influence of pH on the release rate was investigated by performing a set of experiments on the micelles formed from the polymers. Micelles obtained through the dialysis method were stable above pH = 7.4; when the pH was decreased below 7, the degree of ionization of p(His) block of p(HEMA)-*b*-p(His) increased, and at a critical degree of ionization, the hydrophobic interactions weakened, favoring the drug release. Moreover, the enhanced solubility of the p(HEMA) corona also increases under acidic conditions, which helps to diffuse the drug to the external medium.

The drug-release profiles under different pH conditions are compared in Figure 2, realizing the release performance is sensitive to pH and block length of p(His). At lower pH 5.5, the initial release rate is faster than higher pH 7.4, and the total amount of release after 100 h is also found to be faster at pH 5.5 than at pH 7.4. In addition they decrease monotonously in order of $p(HEMA)_{25}$-*b*-$p(His)_{45}$ > $p(HEMA)_{25}$-*b*-$p(His)_{35}$ > $p(HEMA)_{25}$-*b*-$p(His)_{25}$ > $p(HEMA)_{25}$-*b*-$p(His)_{15}$, demonstrating the chain length of His block plays an important role in controlling the release property. p(His) block is an ionizable basic polymer, so its swelling behavior greatly depends on the pH due to the ionization–deionization of the imidazole ring on the p(His) block. At acidic pH values, the p(His) blocks is ionized and the charged imidazole groups repel each other such that this leads to high swelling. The stability of the Dox molecules also is enhanced due its ionization at the low pH environment and results in an increased diffusivity averting all nonbonding interactions with the polymer walls. Our results revealed the pH dependency of the block copolymer can be tailored within certain range by variations of the block size, especially p(His) block, of the copolymers.

2.6. Cytotoxicity of p(HEMA)-*b*-p(His) Micelles

The cytotoxicity of the nanosized micelles of p(HEMA)-*b*-p(His) at various concentrations towards 293T cells and HCT-116 cells

© 2012 WILEY-VCH Verlag GmbH & Co. KGaA, Weinheim

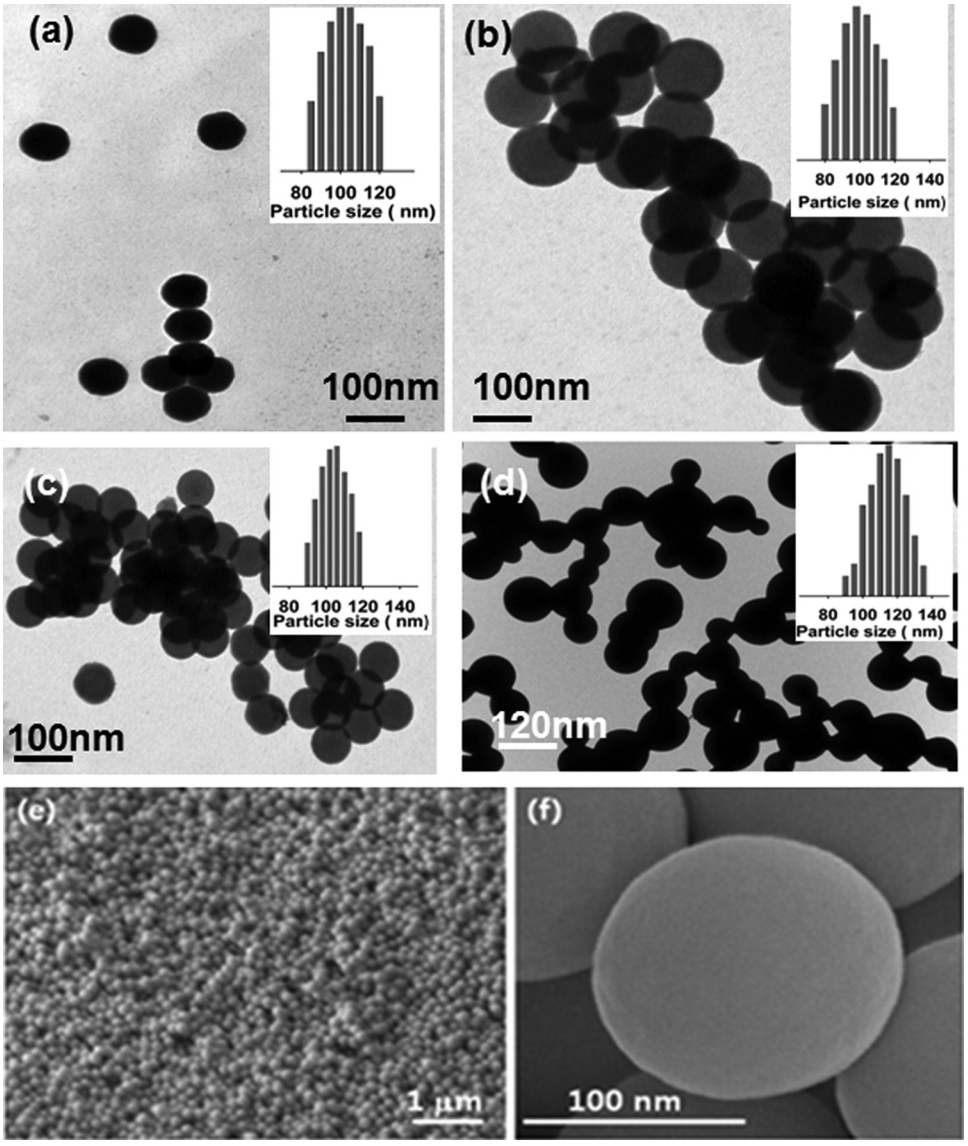

Figure 1. TEM images of the spherical micelles of p(HEMA)-*b*-p(His) obtained from DMSO/DMF-H_2O solution mixture after dialysis: a) $p(HEMA)_{25}$-*b*-$p(His)_{15}$, b) $p(HEMA)_{25}$-*b*-$p(His)_{25}$, c) $p(HEMA)_{25}$-*b*-$p(His)_{35}$, and d) $p(HEMA)_{25}$-*b*-$p(His)_{45}$, and SEM images (e,f) of the Dox-encapsulated spherical micelles fabricated by $p(HEMA)_{25}$-*b*-$p(His)_{35}$. DLS spectra are also shown in inset of TEM images.

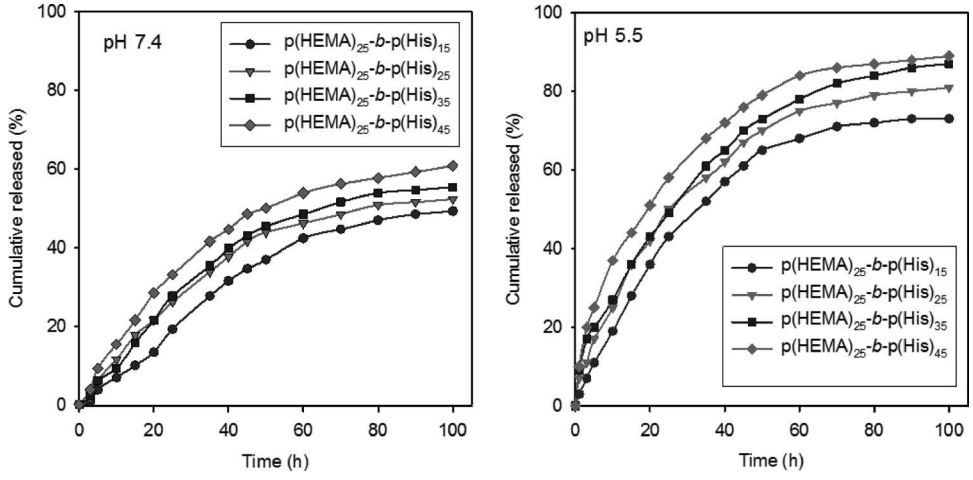

Figure 2. The time-dependent release of Dox from the p(HEMA)-*b*-p(His) micelles fabricated by self-assembly in phosphate-buffered saline (PBS) at 37 °C.

© 2012 WILEY-VCH Verlag GmbH & Co. KGaA, Weinheim

were determined by thiazolyl blue tetrazolium bromide (MTT) cell proliferation assay. The absorbance of a formazan crystal at 560 nm could reflect the number of living cells. It showed a direct proportion relation between absorbance and cell numbers in a reasonable linear range. The cell viability percent was average absorbance of polymer micelles group at different concentrations divided by that of corresponding control group. In this study, the cell-only group was used as control in each experiment, the absorbance of which was similar among eight parallel experiments. Compared to control, the viability of 293T and HCT-116 cells was higher than 80% in a wide concentration range from 1 to 50 μg mL^{-1} (**Figure 3**). At a micelle concentration of 1 μg mL^{-1}, the viability of cells decreases in order of p(HEMA)$_{25}$-*b*-p(His)$_{45}$ > p(HEMA)$_{25}$-*b*-p(His)$_{35}$ > p(HEMA)$_{25}$-*b*-p(His)$_{15}$ > p(HEMA)$_{25}$-*b*-p(His)$_{25}$; however, the order changes to p(HEMA)$_{25}$-*b*-p(His)$_{35}$ > p(HEMA)$_{25}$-*b*-p(His)$_{45}$ > p(HEMA)$_{25}$-*b*-p(His)$_{25}$ > p(HEMA)$_{25}$-*b*-p(His)$_{15}$ at 50 μg mL^{-1}, demonstrating no significant differences among polymer micelles with different lengths of p(His) are found in cytotoxicity against both cells. These results show that p(HEMA)-*b*-p(His) micelles fabricated by self-assembly have no acute and intrinsic cytotoxicity against normal cells.

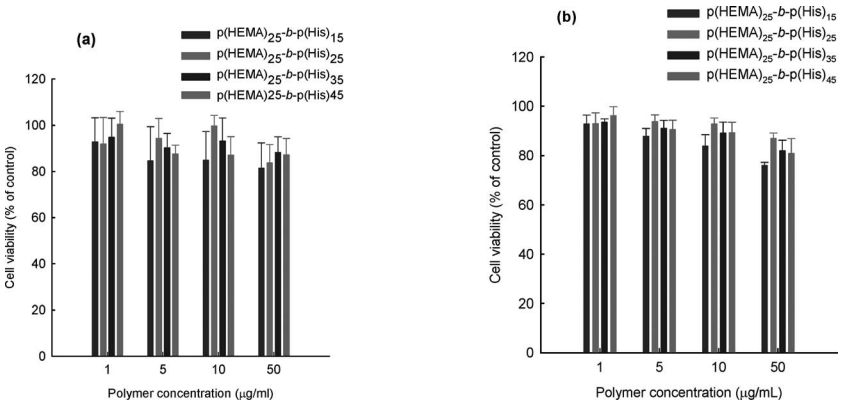

Figure 3. Cytotoxicity of the nano-sized micelles of p(HEMA)-*b*-p(His) at various concentrations towards a) 293T cells and b) to HCT116 normal cells. The cell viability percent was average absorbance of polymer micelles group at different concentrations divided by that of corresponding control (cell-only) group. The absorbance was similar among eight parallel experiments.

2.7. Cellular Uptake and Cytotoxicity of Dox-Loaded p(HEMA)-*b*-p(His) Micelles

To investigate the effect of block copolymer micelles carrying Dox in the cellular level, we incubated the four different Dox-loaded p(HEMA)-*b*-p(His) micelles fabricated by self-assembly with HCT-116 human colon carcinoma cells for 48 h. Dox-loaded micelles showed dose-dependent cytotoxicity at all treatments (**Figure 4**). It is interesting to note that the Dox-loaded p(HEMA)-*b*-p(His) micelles have obvious pH sensitivity and tumor cell survivability by Dox, according to the tests performed by Dox-loaded micelles under various pH conditions (pH 6.0–7.4).

As clearly shown in Figure 4e, the free Dox molecule itself shows decreased antitumor activity at acidic pH 6.0 rather than pH 7.4. The Dox-loaded p(HEMA)-*b*-p(His) micelles showed relatively higher growth inhibition at acidic pH than basic pH at all treatments. Espeicially, at 1 and 10 μg mL^{-1} of Dox concentration, the pH-sensitive cytotoxicity against tumor cells are consistently obtained at all treatment of Dox-loaded p(HEMA)-*b*-p(His) micelles. Comparing the tumor cell survivability at pH 6, the effect of the length of p(His) block on antitumor activity is not conspicuous.

The cells were then observed by confocal laser scanning microscopy (CLSM) in order to get further insight on the pH sensitive endocytosis of the Dox-loaded micelles (**Figure 5**). As expected, stronger fluorescence in cell is clearly observed at acidic pH than basic conditions. For further confirmation, Dox or Dox-loaded micelles treated HCT-116 cells were analyzed using flow cytometer. As shown in **Figure 6**, fluorescence intensity of the Dox-loaded micelles is greatly enhanced at acidic conditions.

Considering the extracellular pH of tumor tissue is acidic (around pH 6.8), pH-sensitive polymeric micelles, specifically at acidic pH have advantages to release the drug into tumor cells. The pH of the tissue and blood stream is about 7.4, Dox-loaded micelles can selectively kill the tumor cells due to the pH-induced destabilization of the micelle and subsequent delivery of the anticancer drug at pH 6.0–6.8.[36] Fluorescence analysis of tumor cells reveled that Dox-loaded micelles showed increased fluorescence intensity at acidic pH while pure Dox showed contrary results, indicating that the Dox-loaded p(HEMA)-*b*-p(His) micelles have tumor-extracellular pH-sensitive targetability. The detailed study on this matter is a facinating topic to be studied in detail and is still on going.

3. Conclusions

We have developed a series of novel biocompatible p(HEMA)-*b*-p(His) hybrid materials by combining ATRP with ROP of His-NCA and evaluated them as pH-sensitive drug-carrier for tumor targeting. Dox can be efficiently loaded into self-assembled micelles of nanoscale and we demonstrated that Dox was released from the micelles in a controlled and sustained manner and that the release rate of Dox was accelerated at low pH 5.5 compared to pH 7.4. The nanosized micelles of p(HEMA)-*b*-p(His) could be effectively internalized by human embryonic kidney 293T cells and HCT116 cells and the viability of both cells was higher than 80% at a micelle concentration range 1 to 50 μg mL^{-1}. The similar nanosized micelles of p(HEMA)-*b*-p(His) bearing Dox molecules could also be effectively internalized by HCT116 carcinoma cells and they slowly released the encapsulated Dox molcules, showing effective cell proliferation inhibition compared to free Dox specifically at an acidic environment. These results suggest that p(HEMA)-*b*-p(His) micelles are promising vehicles to deliver Dox for improved cancer therapy. This work demonstrates

© 2012 WILEY-VCH Verlag GmbH & Co. KGaA, Weinheim

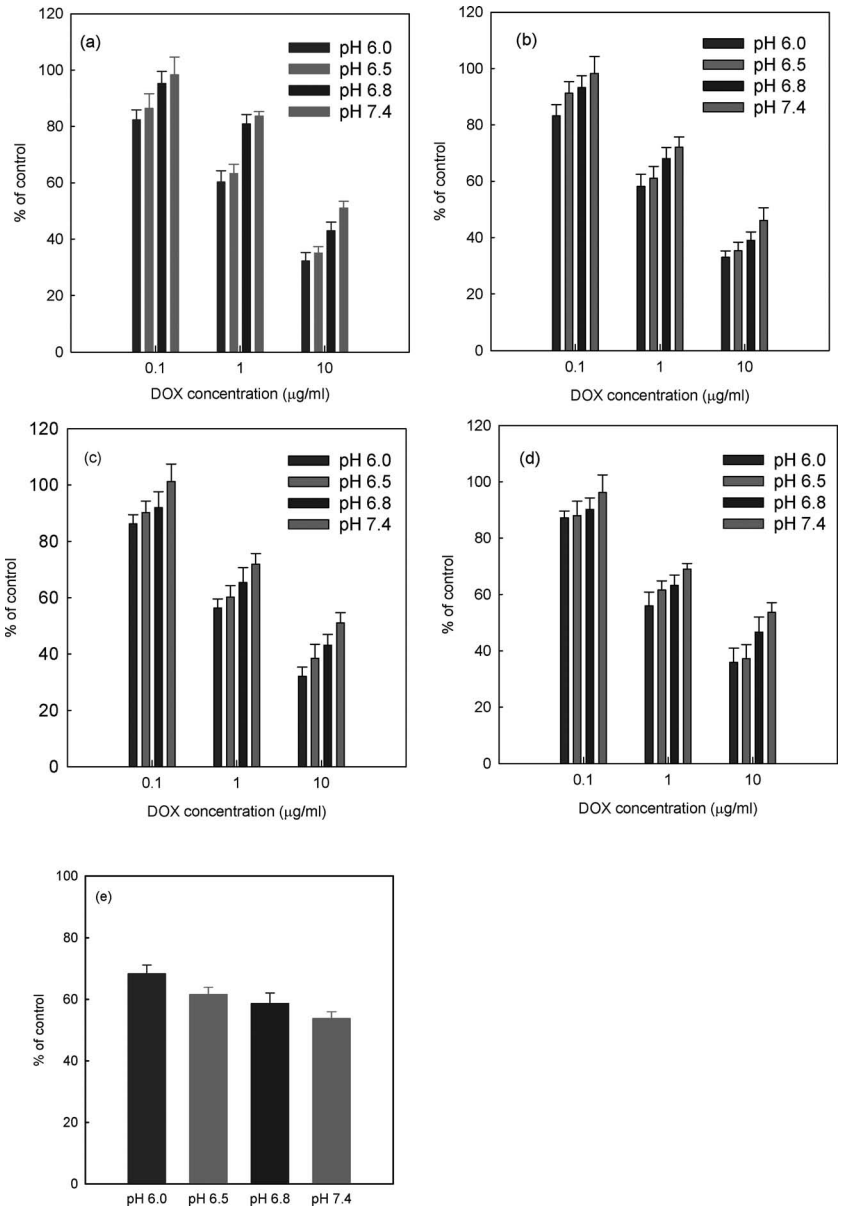

Figure 4. Dose-dependent antitumor activity of Dox-loaded micelles to HCT-116 cells after 48 h incubation: a) $p(HEMA)_{25}$-*b*-$p(His)_{15}$ micelles, b) $p(HEMA)_{25}$-*b*-$p(His)_{25}$ micelles, c) $p(HEMA)_{25}$-*b*-$p(His)_{35}$ micelles, and d) $p(HEMA)_{25}$-*b*-$p(His)_{45}$ micelles. Antitumor activity of free Dox (10 μg Dox mL^{-1}) according to pH at the same incubation time is given in (e). Clear pH-sensitivity of p(HEMA)-*b*-p(His) micelles to antitumor activity can be observed.

that the synthesis of pH-sensitive synthetic polymer bioconjugate hybrid materials is truly biocompatible and they are able to self-assemble in to nanomicelles, which make the new p(HEMA)-*b*-p(His) polymers have a great potential as encapsulants in biomedical domains.

4. Experimental Section

Synthesis of p(HEMA)-Br: p(HEMA) bearing bromide end groups (p(HEMA)-Br) was synthesized by ATRP employing the literature method.[30] Polymerization procedure is described in detail in the Supporting Information. The modification of p(HEMA)-Br to phthalimide end-capped p(HEMA) (p(HEMA)-PI) was carried out according to the literature procedure[37] (also see Scheme 1). p(HEMA) (1.0 g, 0.95 mmol) and phthalimide potassium salt (0.21 g, 1.15 mmol) were heated in refluxing DMF (5 mL) for 8 h. The solvent was removed under high vacuum, washed, and subsequently dried under vacuum at 60 °C for one day. p(HEMA)-PI was obtained in 65% yield.

p(HEMA)-PI (0.30 g, 0.28 mmol) and potassium hydroxide (157 mg, 2.80 mmol) were heated in refluxing *tert*-butyl alcohol (10 mL) for 12 h. After evaporation of the solvent, 10 mL of water was added. The obtained aqueous phase was acidified to pH = 2, extracted with dichloromethane (4 × 5 mL) and then lyophilized, to produce p(HEMA)-NH_2 in 70% yield. For the conversion of p(HEMA)-NH_2 to p(HEMA)-*N*-TMS-amine, p(HEMA)-NH_2 (0.216 g, 0.15 mmol) was dissolved in anhydrous DMF (3 mL) in a 25-mL Schlenk flask, and then BSA (1 mL, 4 mmol) was added. The reaction mixture was stirred for two days. Anhydrous hexane (10 mL) was added to the reaction mixture to precipitate the product. The product was washed with anhydrous hexane and dried under vacuum to produce p(HEMA)-*N*-TMS-amine in a quantitative yield.

The ROP of Bn-His-NCA and Deprotection: Bn-His-NCA was first synthesized for the ROP (see Scheme 1). Boc-L-His(Bn)-OH (2.5 g) was suspended in anhydrous 1,4-dioxane (10 mL), to which a solution of PCl_5 (1.8 g) in 1,4-dioxane (20 mL) was added to form the Bn-His-NCA at 25 °C under stirring. Within a few minutes, a clear solution was obtained, which was then filtered through a glass filter. Crystals of Bn-His-NCA were obtained after the addition of the filtrate to an excess of diethyl ether. The product was subsequently washed and dried under vacuum. For the ROP of Bn-His-NCA by using $p(HEMA)_{25}$-*N*-TMS-amine as a macroinitiator, the $p(HEMA)_{25}$-*N*-TMS-amine (0.45 g, 0.15 mmol) and prescribed amount of Bn-His-NCA were dissolved in DMF in two separate Schlenk flasks and subsequently combined using a transfer needle under nitrogen. The reaction mixture was stirred for 48 h at room temperature under a nitrogen atmosphere. After polymerization, the solvent was concentrated under high vacuum. The concentrated DMF solution was precipitated in anhydrous diethyl ether and dried under vacuum to yield $p(HEMA)_{25}$-*b*-$p(Bn\text{-}His)_n$ (n = 15, 25, 35, 45).

For the deprotection of the benzyl groups, a round-bottomed flask was charged with a solution of the $p(HEMA)_{25}$-*b*-$p(Bn\text{-}His)_n$ in trifluoroacetic acid (100 mg, 3 mL). Then, a four-fold molar excess of a 33 wt% solution of HBr in acetic acid was added, and the reaction mixture was stirred for 2 h at 0 °C. Finally, the reaction mixture was precipitated in anhydrous diethyl ether, and the product was subsequently dried under vacuum to yield $p(HEMA)_{25}$-*b*-$p(His)_n$ (n = 15, 25, 35, 45).

Characterization: ^{1}H NMR spectra were recorded on a Varian Unity Plus-300 spectrometer. Ultraviolet-visible (UV-vis) spectroscopic analysis was performed on a Shimadzu UV-1650 PC, and FTIR spectra were recorded on a Shimadzu IR prestige 21 spectrometer at room temperature. The spectra were taken in KBr discs in the range of 3500–500 cm^{-1}. The MW and PDI of the polymers were determined by GPC with two Styragel columns (HT3 and HT4, Waters Co.) at 40 °C. DMF

© 2012 WILEY-VCH Verlag GmbH & Co. KGaA, Weinheim

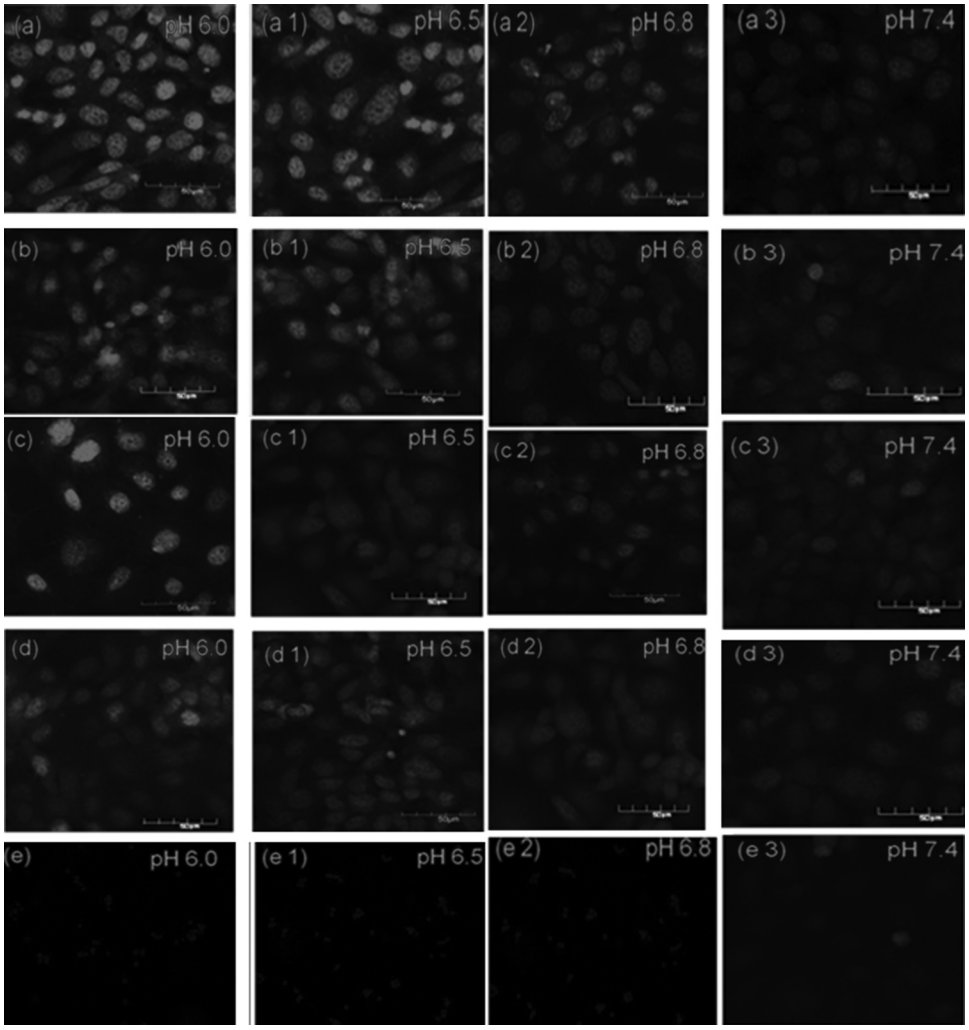

Figure 5. CLSM images of HCT-116 cells after 3 h incubation taken at different pH conditions with Dox loaded p(HEMA)$_{25}$-*b*-p(His)$_{15}$ micelles (a-a3), p(HEMA)$_{25}$-*b*-p(His)$_{25}$ (b-b3), p(HEMA)$_{25}$-*b*-p(His)$_{35}$ (c-c3), p(HEMA)$_{25}$-*b*-p(His)$_{45}$ (d-d3), and free Dox (e-e3) (Dox = 10 μg mL^{-1}). Scale bar = 50 μm.

containing 0.1 N LiBr was used as a carrier solvent at a flow rate of 1.0 mL min^{-1}. A Waters 1515 pump and a Waters 2414 differential refractive index detector were used. Monodispersed PS polymers were used as calibration standards. The micelle particle size was measured by static light scattering (SLS) on a Zetasizer Nano ZS90 (Malvern Instruments, Ltd., U.K.) with a He-Ne laser (633 nm) and 90° collecting optics. The polymeric micelle samples were filtered through a 0.45-μm aqueous membrane filter prior to measurements. Particle size and morphology determination were performed by using electron microscopy. TEM was performed using a JEOL-1299EX TEM with an accelerating voltage of 80 keV. Samples were prepared by pipetting a drop of micelle solution onto a 230-mesh copper grid covered with a Formvar support film that had been pre-coated with a thin film of carbon. After 1 min, the excess solution was blotted away using a strip of filter paper. The samples were left to dry at room temperature for 3 h prior to observation. The SEM images of the nanomicelles were taken with a JEOL-FESEM (JSM-6700F).

Preparation of the Micelles: Micelles were prepared by combining self-assembly with the dialysis method. p(HEMA)-*b*-p(His) (10 mg) was dissolved in DMSO and DMF [5 mL (4/1 v/v)] and stirred for 24 h at 50 °C. Deionized water was then added to the polymer solution at the rate of one drop every 10 s with vigorous stirring until water content reached 25% of the original solution by volume and was heated to 110 °C for 2 h. The clear solution mixture was then allowed to cool down slowly at a rate of 1 °C min^{-1} in an automated thermal-cycler. The slightly turbid solution was transferred into dialysis membrane tubing (MEMBRA-CEL MD34-7, MW cutoff = 1000) and dialyzed for 48 h against NaOH/$Na_2B_4O_7$ buffer (pH 7.4, 20 mM) to remove organic solvents. The outer phase was replaced at 6 h intervals with fresh buffer. The solution was subsequently lyophilized after filtering through a 0.8-μm syringe filter in order to remove any impurities and non-micellar aggregates. The preparation of Dox-loaded micelles was similar to that of the p(HEMA)-*b*-p(His) micelles except the addition of a predetermined amount of Dox in DMSO and DMF (4/1 v/v) solution.

Determination of Drug Loading Content (DLC) and Efficiency (DLE) and In Vitro Drug Release: For the quantification of the amount of drug encapsulated, aliquots of the drug-loaded micelle solution were lyophilized and broken up by adding 2 mL of DMSO. The obtained solution was analyzed using the UV-vis spectroscopy. The characteristic absorbance of Dox (485 nm) was recorded and compared with a standard curve generated in DMF of drug concentrations varying from 0–100 mg mL^{-1}. The percentages of DLC and DLE were calculated according to the following equations: DLC [%] = (weight of drug in the

© 2012 WILEY-VCH Verlag GmbH & Co. KGaA, Weinheim

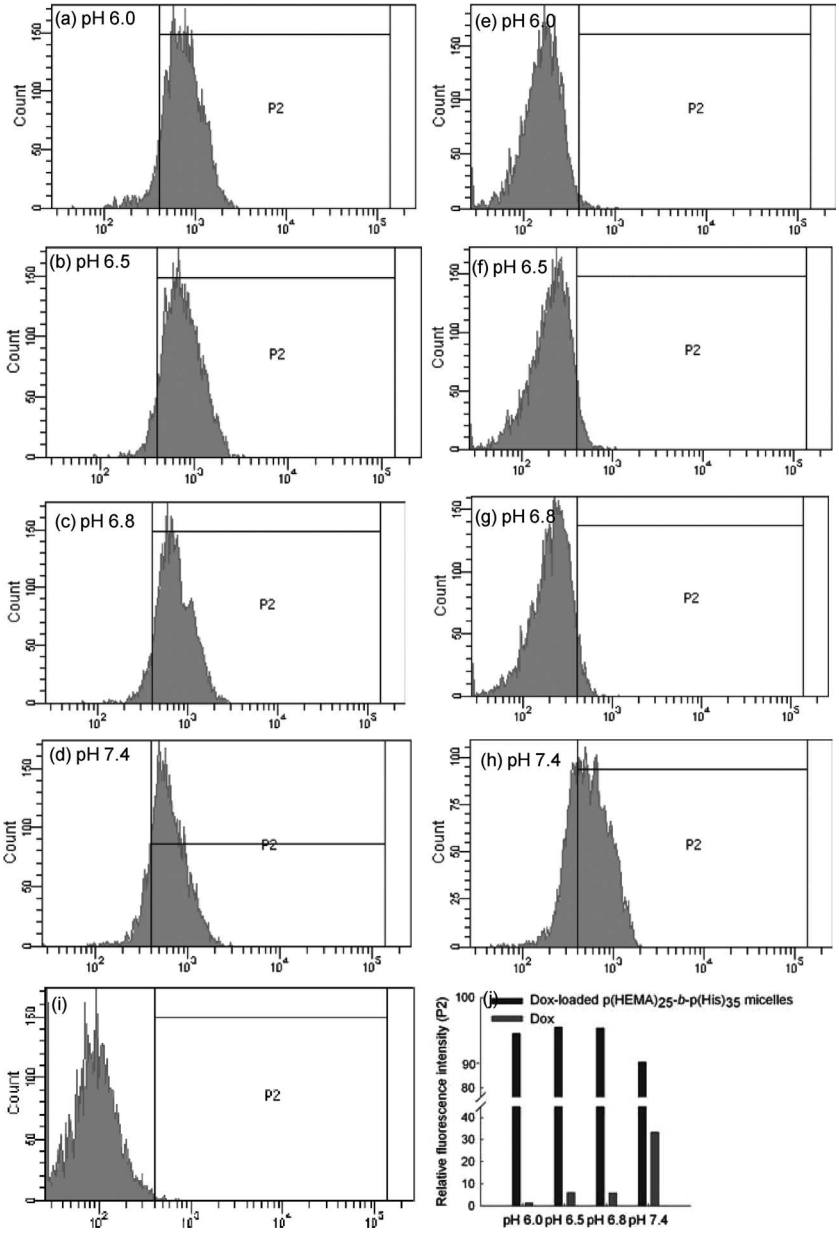

Figure 6. Flow cytometric analysis of HCT-116 cells after the exposure to Dox-loaded micelles of $p(HEMA)_{25}$-*b*-$p(His)_{35}$ (a–d) and free Dox (10 μg mL^{-1}) (e–h) at different pH conditions for 3 h. The controls were plotted in (i) and (j). 1.0×10^6 Cells were used for FACS scan analysis.

micelle/weight of drug loaded micelle) × 100 and DLE [%] = (weight of drug in the micelle/weight of drug for drug loaded micelle preparation) × 100.

For in vitro drug release, a fixed amount of Dox-loaded micelle solution suspended in dialysis bags was placed into buffer solution (PBS, 20 mL) with the required pH value. Then, the samples were placed in a shaking bath at 70 rpm and at the required temperature. The buffer solution was periodically replaced with a fresh solution and the amount of released drug was measured by UV-vis spectroscopy. The drug concentration was determined according to the standard curves for the drug solution at different pH values.

Cell Culture and Confocal Laser Scanning Microscopy (CLSM): HCT-116 human colon carcinoma cells were cultured in RPMI-1640 medium supplemented with 10% fetal bovine serum, at 37 °C and 5% CO_2 atmosphere. HCT116 cells were seeded in a 6-well plates with 1000 μL of medium and then incubated overnight in a CO_2 incubator (5% CO_2) at 37 °C. Twenty four hours later, free Dox or Dox-loaded micelles were added to the cells and incubated for 3 h. Cells were then washed with PBS (pH 7.4, 0.1 M) and treated with 4% paraformaldehyde and fixed by immobilization solution (IMMU-MOUNT, Thermo Electron Corporation). These cells were observed with a CLSM (Leica TCS-SP2).

Cytotoxicity Studies and Flow Cytometer Analysis: Human embryonic kidney 293T (293T) cells and HCT-116 normal cells were used to confirm cytotoxicity of the nanosized micelles of p(HEMA)-*b*-p(His). Both cells were maintained in RPMI-1640 medium supplemented with 10% fetal bovine serum (5% CO_2 at 37 °C). Viability of the cells were evaluated by thiazolyl blue tetrazolium bromide (MTT) cell proliferation assay. 2×10^4 cells seeded in 96-well plates with 100 μL of medium were incubated overnight in a CO_2 incubator (5% CO_2 at 37 °C) and then media was exchanged with 100 μL of serum-free RPMI1640 media. For cytotoxicity test, p(HEMA)-*b*-p(His) micelles were distributed in serum-free RPMI1640 media and diluted to appropriate concentrations. After 2 day of incubation, 30 μL of MTT (5 mg mL^{-1}) was added to 96-well plates and incubated for 4 h. The formazan crystals formed were solubilized in DMSO, and the absorbance (560 nm-test/630 nm-reference) was determined using an automated computer-linked microplate reader (Molecular Device Co. U.S.A.). The results were expressed as a percentage of absorbance compared to that in the control cells. Each measurement was obtained as the mean value of eight wells and all experiments were conducted in triplicate.

The cytotoxicity of Dox-loaded micelles and free Dox were measured aginst HCT-116 colon carcinoma cells by MTT cell proliferation assay. The cells were seeded in a 96-well plates at the density of 5×10^3 cells per well and incubated in 100 μL of medium at 37 °C in 5% CO_2 for 24 h. Then the medium was removed and replaced with (100 μL) free Dox or Dox-loaded micelles containing medium. Controls were treated with 0.5% v/v of DMSO. After 48 h incubation, 30 μL of MTT (5 mg mL^{-1} in PBS) was added to 96-well plates, followed by incubation for 4 h. The formazan crystals formed were solubilized with 100 μL DMSO, and the absorbance (560 nm-test/630 nm-reference) was determined using an automated computer-linked microplate reader (Molecular Device Co.) and the relative cell viability was calculated.

For flow cytometer analysis, Dox or Dox-loaded micelles treated HCT 116 cells were seeded at a density of 1×10^6 cells in 6-well plates and incubated overnight. Dox or Dox-loaded micelles (10 μg Dox mL^{-1}) were added and incubated for 3 h. Cells were harvested and analyzed with a flow cytometer (FACScan). An excitation wavelength at 488 nm and emission wavelength at 522 nm were used to observe the Dox fluorescence intensity.

Supporting Information

Supporting Information is available from the Wiley Online Library or from the author.

© 2012 WILEY-VCH Verlag GmbH & Co. KGaA, Weinheim

Acknowledgements

This work was supported by grants-in-aid for the World Class University Program (No. R32-2008-000-10174-0) and the National Core Research Center Program from MEST (No. R15-2006-022-01001-0), and the Brain Korea 21 program (BK-21).

Received: November 15, 2011
Published online: December 23, 2011

[1] a) E. P. Holowka, D. J. Pochan, T. J. Deming, *J. Am. Chem. Soc.* **2005**, *127*, 12423; b) J. R. Hernandez, S. Lecommandoux, *J. Am. Chem. Soc.* **2005**, *127*, 2026.
[2] J. N. Cha, G. D. Stucky, D. E. Morse, T. J. Deming, *Nature* **2000**, *403*, 289.
[3] R. Savic, L. Luo, *Science* **2003**, *300*, 615.
[4] D. L. Elbert, C. B. Herbert, J. A. Hubbell, *Langmuir* **1999**, *15*, 5355.
[5] H. G. Schild, *Prog. Polym. Sci.* **1992**, *17*, 163.
[6] Q. Cai, K. Zeng, C. Ruan, T. A. Desai, C. A. Grimes, *Anal. Chem.* **2004**, *76*, 4038.
[7] J. Virtanen, M. Arotcarena, B. Heise, S. Ishaya, A. Laschewsky, H. Tenhu, *Langmuir* **2002**, *18*, 5360.
[8] a) G. D. Poe, W. L. Jarrett, C. W. Scales, C. L. McCormick, *Macromolecules* **2004**, *37*, 2603; b) Y. Mei, K. L. Beers, H. C. M. Byrd, D. L. van der Hart, N. R. Washburn, *J. Am. Chem. Soc.* **2004**, *126*, 3472; c) H. Rettig, E. Krause, H. G. Borner, *Macromol. Rapid Commun.* **2004**, *25*, 1251; d) C. M. Dong, X. L. Sun, K. M. Faucher, R. P. Apkarian, E. L. Chaikof, *Biomacromolecules* **2004**, *5*, 224; e) D. Bontempo, H. D. Maynard, *J. Am. Chem. Soc.* **2005**, *127*, 6508; f) M. G. J. ten Cate, H. Rettig, K. Bernhardt, H. G. Borner, *Macromolecules* **2005**, *38*, 10643; g) C. Boyer, V. Bulmus, J. Liu, T. P. Davis, M. H. Stenzel, C. B. Kowollik, *J. Am. Chem. Soc.* **2007**, *129*, 7145; h) K. R. Brzezinska, T. J. Deming, *Macromol. Biosci.* **2004**, *4*, 566.
[9] N. Hadjichristidis, H. Iatrou, M. Pitsikalis, G. Sakellariou, *Chem. Rev.* **2009**, *109*, 5528.
[10] H. A. Klok, S. Lecommandoux, *Adv. Polym. Sci.* **2006**, *202*, 75.
[11] G. Floudas, P. Papadopoulos, H. A. Klok, G. W. M. Vendermeulen, J. R. Hernandez, *Macromolecules* **2003**, *36*, 3673.
[12] C. He, C. Zhao, X. Chen, Z. Guo, X. Zhuang, X. Jing, *Macromol. Rapid. Commun.* **2008**, *29*, 490.
[13] C. M. Kania, H. Nabizadeh, D. G. McPhillimy, R. A. Patsiga, *J. Appl. Polym. Sci.* **1982**, *27*, 139.
[14] S. Ludwigs, G. Krausch, G. Reiter, M. Losik, M. Antonietti, H. Schlaad, *Macromolecules* **2005**, *38*, 7532.
[15] A. Nakajima, K. Kugo, T. Hayashi, *Macromolecules* **1979**, *12*, 844.
[16] R. Yoda, S. Komatsuzaki, E. Nakanishi, T. Hayashi, *Eur. Polym. J.* **1995**, *31*, 335.
[17] L. Rubatat, X. Kong, S. A. Jenekhe, J. Ruokolainen, M. Hojeij, R. Mezzenga, *Macromolecules* **2008**, *41*, 1846.
[18] L. M. Seifert, R. T. Green, J. Biomed. *Mater. Res.* **1985**, *19*, 1043.
[19] H. S. Bennet, A. D. Wyricks, S. W. Lee, H. McNeil, *J. Stain Technol.* **1976**, *51*, 71.
[20] a) T. Canal, N. A. Peppas, J. Biomed. *Mater. Res.* **1989**, *23*, 1183; b) M. Mijajima, T. Okano, S. W. Kim, W. Higushi, *J. Controlled Release* **1987**, *5*, 179.
[21] a) C. Pichon, C. Goncalves, P. Midoux, *Adv. Drug Delivery Rev.* **2001**, *53*, 75; b) J. M. Benns, J. S. Choi, R. I. Mahato, J. S. Park, S. W. Kim, *Bioconjugate Chem.* **2000**, *11*, 637.
[22] a) R. Cortesi, E. Esposito, E. Menegatti, R. Gambari, C. Nastruzzi, *Int. J. Pharm.* **1994**, *105*, 181; b) T. Alexakis, D. K. Boadi, D. Quong, A. Groboillot, I. O'Neill, D. Poncelet, R. J. Neufeld, *Appl. Biochem. Biotechnol.* **1995**, *50*, 93.
[23] a) B. Ekman, I. Sjoeholm, *J. Pharm. Sci.* **1978**, *67*, 693; b) J. S. Choi, E. J. Lee, S. J. Park, H. J. Kim, J. S. Park, *Bull. Korean Chem. Soc.* **2001**, *22*, 261; c) E. G. Bellomo, M. D. Wyrsta, L. Pakstis, D. J. Pochan, T. J. Deming, *Nat. Mater.* **2004**, *3*, 244; d) F. Checot, A. Brulet, J. Oberdisse, Y. Gnanou, O. Mondain-Monval, S. Lecommandoux, *Langmuir* **2005**, *21*, 4308.
[24] S. Abraham, C.-S. Ha, I. Kim, *J. Polym. Sci. Part A: Polym. Chem.* **2006**, *44*, 2774.
[25] a) R. Jeyanthi, K. P. Rao, *J. Controlled Release* **1990**, *13*, 91; b) S. Abraham, S. Brahim, K. Ishihara, A. Guiseppi-Elie, *Biomaterials* **2005**, *26*, 4767; c) A. Denizli, A. Tuncel, M. Olcay, V. Sarnatskaya, V. Sergeev, V. G. Nikolaev, E. Piskin, *Clin. Mater.* **1992**, *11*, 129.
[26] a) D. Y. Sogah, W. R. Hertler, O. W. Webster, G. L. Cohen, *Macromolecules* **1987**, *20*, 1473; b) Y. Nagasaki, H. Ito, M. Kato, K. Kataoka, T. Tsuruta, *Polym. Bull.* **1995**, *35*, 137.
[27] J. S. Wang, K. Matyjaszewski, *J. Am. Chem. Soc.* **1995**, *117*, 5614; b) M. Kato, M. Kamagaito, M. Sawamoto, T. Higashimura, *Macromolecules* **1995**, *28*, 1721.
[28] K. Matyjaszewski, J. Xia, *Chem. Rev.* **2001**, *101*, 2921.
[29] a) J. V. M. Weaver, I. Bannister, K. L. Robinson, X. B. Azeau, S. P. Armes, M. Smallridge, P. McKenna, *Macromolecules* **2004**, *37*, 2395.
[30] K. L. Beers, S. Boo, S. G. Gaynor, K. Matyjaszewski, *Macromolecules* **1999**, *32*, 5772.
[31] T. J. Deming, *J. Am. Chem. Soc.* **1998**, *120*, 4240.
[32] I. Dimitrov, H. Schlaad, *Chem. Commun.* **2003**, 2944.
[33] T. Aliferis, H. Iatrou, N. Hadjichristidis, *Biomacromolecules* **2004**, *5*, 1653.
[34] a) H. Lu, J. Cheng, *J. Am. Chem. Soc.* **2007**, *129*, 14114; b) H. Lu, J. Cheng, *J. Am. Chem. Soc.* **2008**, *130*, 12562.
[35] G. Riess, *Prog. Polym. Sci.* **2003**, *28*, 1107.
[36] a) E. S Lee, H.J. Shin, K. Na, Y. H. Bae, *J. Controlled Release* **2003**, *90,* 363; b) E.S Lee, Y. S.Youn, *Bull. Korean Chem. Soc.* **2008**, *29*, 1539.
[37] S. Monge, O. Giani, E. Ruiz, M. Cavalier, J. J. Robin, *Macromol. Rapid Commun.* **2007**, *28*, 2272.

© 2012 WILEY-VCH Verlag GmbH & Co. KGaA, Weinheim